

Molecular Dynamics Simulation of Sodium Dodecyl Sulfate Micelle in Water: Micellar Structural Characteristics and Counterion Distribution

Chrystal D. Bruce[†], Max L. Berkowitz,* Lalith Perera[‡], and Malcolm D. E. Forbes[§]

Department of Chemistry, University of North Carolina at Chapel Hill, CB#3290 Venable and Kenan Labs, Chapel Hill, North Carolina 27514

Received: September 25, 2001; In Final Form: January 3, 2002

An all-atom 5 nanosecond molecular dynamics simulation of a water-solvated micelle containing 60 sodium dodecyl sulfate monomers was performed. Structural properties such as the radius of gyration, eccentricity, micellar size, accessible surface area, dihedral angle distribution, carbon atom distribution, and the orientation of the monomers toward the micelle center of mass were evaluated. The results indicate a stable micellar system over the duration of the simulation. Evaluation of the structure and motion of the sodium counterions show (1) a long equilibration time (1 nanosecond) is required to achieve a stable distribution of counterions and (2) approximately 25% of the sodium ions are located in the first shell and 50% are located in the first two shells of the micelle during the course of the simulation. The structure of the micelle oxygen–sodium ion radial distribution function reveals two distinct peaks which divide the counterions into those close to the micelle (first shell) those far from the micelle (bulk) and those between (second shell). Finally, values of the diffusion coefficient for sodium ions followed a decreasing trend for ions in the bulk of the micellar system ($D = 1.9 \times 10^{-5} \text{ cm}^2/\text{s}$), ions in the second shell of the micelle ($D = 1.4 \times 10^{-5} \text{ cm}^2/\text{s}$), and those in the first shell of the micelle ($D = 1.0 \times 10^{-5} \text{ cm}^2/\text{s}$).

Introduction

Surfactants have long been of importance as cleaning agents, as components of polymerization processes, and as models of biological systems. They have been extensively analyzed using a variety of experimental and theoretical techniques including NMR,^{1–5} EPR,^{6–8} light scattering,^{9,10} small angle neutron scattering,^{11,12} Monte Carlo simulations^{13,14} and molecular dynamics (MD) simulations.^{15–25} It is important to understand the physical properties of micelles from the perspective of organized assemblies and their use as solubilizing agents.

With recent increases in computing power, MD simulations of micelles have seen a resurgence.^{23,26,27} Bogusz et al.²⁶ performed simulations of nonionic octyl glucoside micelles with sizes ranging from 1 to 75 surfactant molecules per micelle. They found that micelles consisting of 10 or more monomers were stable over the course of their 4 nanosecond simulations. To date, there has not been a significant number of simulations of this category of surfactants. This is also true of zwitterionic surfactants. In 1989, Wendoloski et al. reported on a 100 picosecond simulation of a lysophosphatidylethanolamine (LPE) phospholipid micelle. More recently, Tieleman et al.²³ studied micelles formed from the zwitterionic molecule dodecylphosphocholine (DPC). Analysis of the last 500 ps for simulations of 40, 54, and 65 monomer micelles revealed differences in shape, accessible surface area, and monomer packing. The DPC molecule has also been the basis of a molecular dynamics examination of micelle formation conducted by Marrink et al.²⁸ All of these studies have significantly advanced the understanding of the molecular-level structure and dynamics of these two categories of surfactants.

In contrast, over the past 20 years many MD simulations have been performed on ionic surfactant systems, but the systems have, in general, not been as large nor have they been studied on very long time scales. Much of this prior work consists of simulations that are less than 200 ps in duration.^{22,24} In addition, these earlier studies were performed on sodium octanoate which has only 10 heavy atoms and forms micelles that contain approximately 15 monomers, so the number of atoms in the system is much more manageable computationally.^{17,18} Indeed, the computational effort required to properly handle the long range electrostatic forces of larger ionic surfactants has been the primary reason for the lack of larger and longer simulations. Simulation conditions have to be such that the periodic images are not interacting. This requirement results in large systems. In addition, proper treatment of electrostatic forces must be applied so that there are no artifacts from cutoffs and that the true behavior of the highly charged counterions can be determined.²⁹

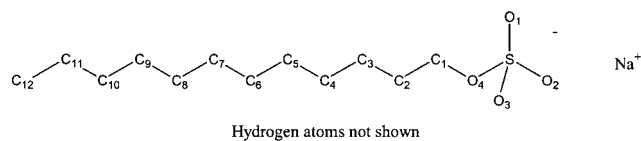
Two investigations into the behavior of the larger ionic surfactant sodium dodecyl sulfate (SDS) have been performed. In 1990, Shelley, Watanabe, and Klein²⁴ reported on a 182 picosecond simulation of a 42 monomer SDS micelle, and, in 1995, MacKerrell²² performed a 120 ps simulation of a 60 monomer SDS micelle. Both of these studies report flexible hydrocarbon tails, stable micelle structure, and low water penetration into the micelle. One of the primary differences in the results of these two simulations, though, is the behavior of the sodium counterions. MacKerrell observes complete dissociation, whereas Shelley et al. find approximately 12% of the sodium ions form contact ion pairs with the micelle during the course of their simulation. Counterion behavior in surfactant systems has long been a topic of debate. Many researchers have concluded that all counterions are dissociated from the micelle

* To whom correspondence should be addressed. maxb@unc.edu.

[†] cbruce@email.unc.edu.

[‡] lalith_perera@unc.edu.

[§] mdef@unc.edu.

SCHEME 1: Structure of Sodium Dodecyl Sulfate (SDS)**TABLE 1: Surfactant Headgroup Charges**

atom	charge (e)
C ₁	0.137
O ₄	-0.459
S	1.284
O ₁₋₃	-0.654
Na ⁺	1
all other atoms	0

and no contact ion pairs exist. Others have reported counterion binding ranging from 40% to 80%.³⁰

Here, we report the results of a 5 nanosecond MD simulation of sodium dodecyl sulfate. (See Scheme 1.) Our system contains 7579 water molecules and 60 SDS molecules for an overall concentration of SDS of 0.4 M. This large number of water molecules allows a more accurate simulation of the environment of the micelle and investigation of the behavior of counterions at the edge of the micelle by providing a large distance between periodic images. In addition, attentive computational handling of the large number of charged species in this system using the Particle Mesh Ewald technique³¹ leads to a more complete and accurate assessment of the behavior of the counterions.³² The size of the system, the treatment of the electrostatic interactions, and the length of the simulation extend the molecular-level knowledge of ionic surfactant systems, in a fashion similar to simulations done recently on nonionic²⁶ and zwitterionic surfactants.²³

Below results are presented pertaining to (1) the structure of the micelle itself and (2) the structural properties of the sodium counterions. The structural and dynamical properties of the water molecules in relation to the micelle and the counterions can be found in a separate publication.³³

Method. Using Insight II software, available from Accelrys Inc., an SDS micelle was built consisting of sixty dodecyl sulfate monomers in the all trans configuration and including explicit hydrogen atoms. The micelle was constructed so that the innermost methyl group in each of the hydrophobic tails was placed at the apex of a “buckyball” with a radius of 3.5 Å, and the remainder of the monomer extending outward as per MacKerrell.²² Because the aggregation number of SDS has been reported to be in the range 60–70 at room temperature,^{30,34} the choice of a 60 monomer micelle is appropriate because it is both small enough to be computationally feasible and large enough to mimic all of the physical properties of the micelle. Additionally, we can make direct comparisons with the previous work of MacKerrell. Charges were assigned to the atoms in the headgroup as defined in Table 1.^{24,35} Extensive equilibration and thermalization of this highly ordered micelle was performed in Insight II using the cvff force field. After adding water to the system, it was determined that due to the nature of the electrostatic interactions, a program with a faster and more accurate method to handle long-range interactions was necessary. Therefore, the trajectory of the micelle without sodium counterions or water and all further simulations were calculated using the program AMBER 6³⁶ and the parm98 force field. Force field parameters for the headgroup atoms were taken from Schweighofer et al.³⁵ The system was then subjected to further minimization and thermalization with the sulfur atoms fixed

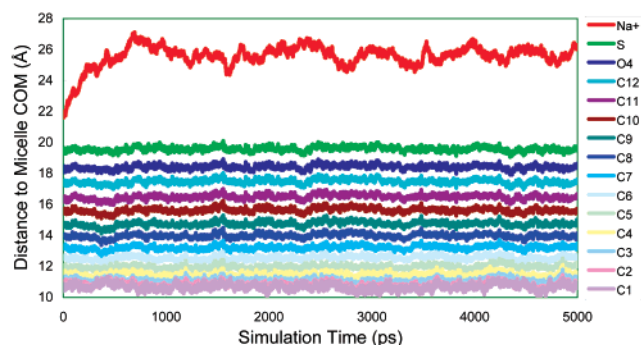


Figure 1. Average distance of selected atoms from the micelle center of mass as a function of simulation time.

followed by the addition of 60 sodium counterions and TIP3P water molecules to provide a 10 Å buffer region between the micelle and the edge of the periodic box. As a result, 7579 water molecules were added bringing the total number of atoms in the system to 25317. Nonbonded cutoffs were fixed at 9 Å, and all long-range electrostatic forces were calculated using the Particle Mesh Ewald technique³¹ included in AMBER 6. The nonbonded atom list was updated when any atom moved more than 5 Å from its position at the last update. Thermalization of the water was carried out with the micelle and Na⁺ cations held fixed. Finally, a 40 ps NPT (P = 1 atm, T = 300 K) simulation was carried out to allow the micelle and water molecules to equilibrate. The final density of the entire system was 1.0051 g/mL (compared to an experimental density of 1.0093 g/mL), and the final box size was 65.042 × 61.762 × 63.348 Å. A 5 nanosecond NVT simulation was carried out at 300 K using SHAKE for all bonds containing hydrogen and the Berendsen temperature coupling method³⁷ with a time parameter of 1.0 ps. A 2 fs time step was used during the production run.

Results and Discussion

As mentioned above, one of the primary differences between this work and all of the earlier MD simulations of ionic surfactants is the length of the simulation. Examination of the average distance of selected atoms to the micelle center of mass as a function of simulation time (Figure 1) shows that a full 1 ns of simulation time is required to reach a stable equilibrium distribution of the sodium counterions in the simulation. As a result, the first nanosecond of the production run has been discarded as a nonequilibrated state. The remainder of the data to be presented here is from the final 4 ns of the simulation. It should be noted that the micelle itself remains stable throughout the course of the entire simulation.

Micelle Structure. Investigation of the structure of the micelle by molecular dynamics provides clues into the macroscopic behavior of surfactant systems. The size and shape adopted by the micelle is important in determining its suitability in polymerization reactions. The mobility of the hydrocarbon chains give indications of how species inside micelles diffuse through the interior. In using surfactants as microreactors, the penetration of water or other polar species is important in the design, synthesis, and development. All of these research areas benefit from the study of micellar structure.

Micelle Shape. The stability of the micelle can be further characterized by examining the eccentricity defined as³⁸

$$e = 1 - \frac{I_{\min}}{I_{\text{avg}}} \quad (1)$$

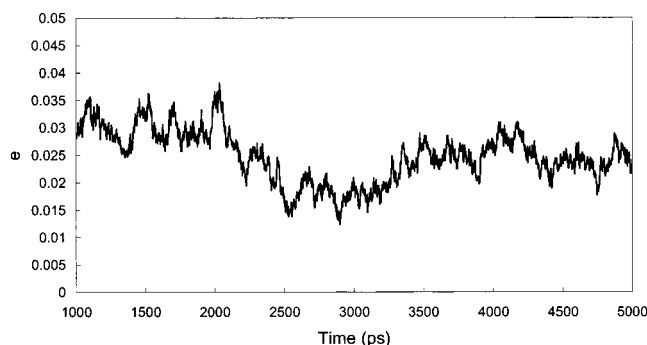


Figure 2. Eccentricity of the micelle over the last 4 ns of the simulation.

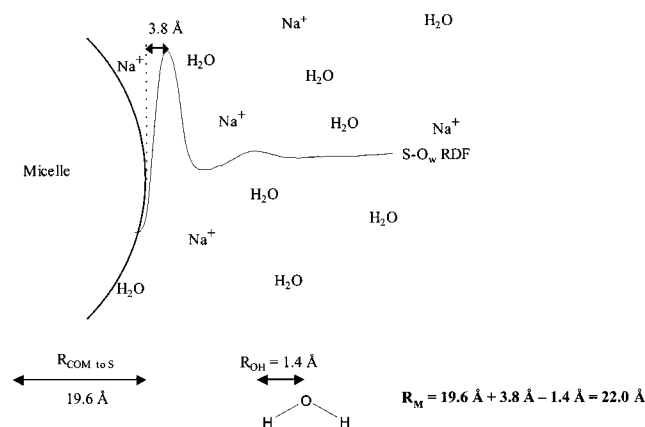


Figure 3. Interface Scheme.

where I_{\min} is the moment of inertia along the x , y , or z axis with the smallest magnitude and I_{avg} is the average of all three moments of inertia. Figure 2 shows the eccentricity as a function of simulation time for the final 4 ns of the production run. For a perfect sphere, the value of e would be zero, so the deviation from a spherical object can be quantified by examining the eccentricity in addition to simple visual inspection of snapshots of the system. It is clear that this is not a perfectly spherical system, but that the micelle shape is stable over the course of the simulation. As a point of comparison, the average value found for I_{\max}/I_{\min} is 1.05 which is in the range reported previously for SDS simulations of 1.13²⁴ and 1.02.²² A value for I_{\max}/I_{\min} of 1.12 and an eccentricity of 0.06 are obtained for a 54 lipid DPC micelle²³ indicating a slightly less spherical micelle.

Micelle Size. One of the primary characteristics of micelle structure is its size. We have chosen to define the radius of the micelle as the average distance of the sulfur atoms of the headgroup to the micelle center of mass (19.6 Å) plus the distance at the first peak of the sulfur to water oxygen radial distribution function (3.8 Å) minus the radius of water (1.4 Å) for an effective micellar radius of 22.0 Å. (See Figure 3.) X-ray scattering gives a micellar radius of 22.3 Å.³⁹ Another method for determining the micellar radius is given in eq 2²⁶

$$R_s = \sqrt{\frac{5}{3}} R_g \quad (2)$$

For the last 4 ns of the simulation, the average radius of gyration, R_g , of the micelle was 16.2 ± 0.12 Å. This gives a micelle radius, R_s , of 20.9 ± 0.15 Å from eq 2. As a point of comparison, MacKerrell reports a value of 19.70 Å for the rms distance of the sulfur atoms to the micelle center of mass and an R_g of 16.02. Bendedouch and Chen¹¹ report a mean micellar

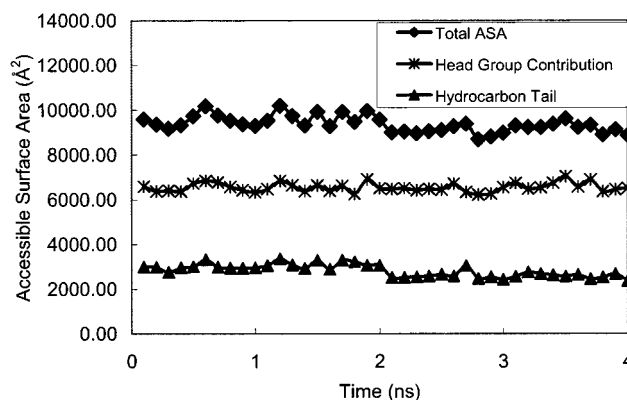


Figure 4. Accessible Surface Areas.

radius of 18.9 Å and an average radius of gyration of 15.4 Å for lithium dodecyl sulfate using small angle neutron scattering.

Accessible Surface Area. An additional analysis that can be performed to study the structural properties of the micelle is to quantify the accessible surface area. The method of Lee and Richards⁴⁰ was used to determine the surface area of the micelle available for interaction with water. In this technique, all of the sodium and water molecules are removed from the system and a probe molecule is rolled across the surface of the micelle and the contact area is summed to quantify the total accessible surface area. A 1.4 Å probe was utilized to mimic the water in the system. It is possible to separate the contribution from the sulfate headgroup and the hydrocarbon tails. The results of this analysis are presented in Figure 4.

As a starting point, the accessible surface area of the initial “buckyball” structure was calculated. The contribution to the surface area from the headgroups is 10 007 Å² and that from the tails is 4323 Å² for a total of 14 330 Å². The actual surface area of the relaxed micelle would be expected to be less than this considering there are gaps between the surfactant chains that create an unrealistically rough surface in the initial structure. Once the micelle has equilibrated and the tails have relaxed, a time averaged value of 10 548 Å² was found for the accessible surface area (or 176 Å² per monomer). This value is comparable to that of 180 Å² per lipid found for a 54 monomer DPC micelle²³ which is approximately the same size as the SDS micelle examined here. The majority of the contribution to the accessible surface area of the micelle comes from the headgroups, although there are occasions where the hydrocarbon tails contribute significantly because there is considerable torsional motion of the chains. See Figure 4. The decrease in surface area from the initial structure is due to conformational relaxation and due to liquifying of the tails, after which they fill the interior of the micelle.

It is interesting to note how the average value for the surface area of the micelle (SA_{micelle}) differs from the total surface area of a perfect sphere (SA_{sphere}) with radius 22 Å which is 6082 Å²: SA_{micelle} is nearly double that of SA_{sphere} due to the surface roughness of the micelle. An additional contribution to surface area is also due to the fact that the micelle is not completely spherical but has an ellipsoidal element. The surface area of an ellipsoid with roughly the same volume as a sphere of radius 22 Å, and the same eccentricity and ratio of I_{\max}/I_{\min} is 7690 Å² or 26% greater. Therefore, in addition to the surface roughness, the nonspherical nature of the micelle contributes to the increased surface area.

Chain Direction. A simple method for evaluating the extent of torsional motion of the micelle is to examine the angle formed

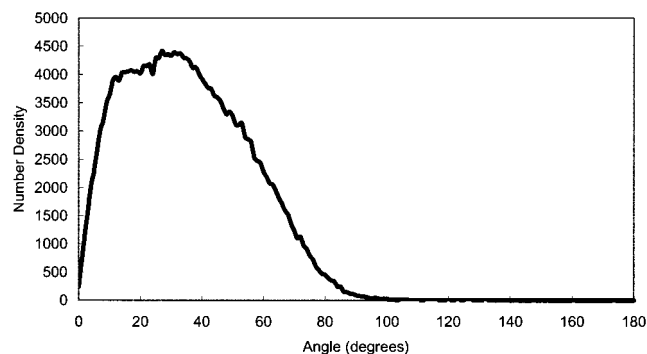


Figure 5. C_{12} , C_1 , COM angle distribution summed over last 4ns of simulation. Analyzed every 1 ps.

by the vector from C_1 (the headgroup carbon) to C_{12} (the carbon of the terminal methyl group) and the vector from C_1 to the micelle center of mass. When this angle is zero, the chain is pointing directly at the center of the micelle (as in the initial setup of the system). As this angle increases, the deviation from a common representation of a micelle as a “wheel with spokes” increases. Figure 5 shows the number of times a given angle was found for each of the surfactant monomers over the last 4 ns of the simulation. This value was evaluated every 1 ps. What is observed is a fairly broad plateau from 12° to 38° . This indicates that, in general, the surfactant monomers are oriented toward the micelle center of mass while not being perfectly pointed at the center as noted in Bogusz et al.²⁶ This can be confirmed by visual examination of cross sections of the micelle (see Figure 6).

Sodium Counterions. It is known from studies of DNA and protein folding that the electrostatic interaction between the positive counterion(s), and these anionic biological species plays a crucial role in determining the structure of the molecule. Depending on the charge and the location of the counterion, DNA may relax into a toroidal shape⁴¹ and proteins have been found to unfold in approximately 100 ps when the treatment of electrostatic long-range forces is not handled properly.^{29,42} The use of the Particle Mesh Ewald technique³¹ in this simulation, as opposed to truncating the long-range electrostatic forces with cutoffs, results in careful and reliable treatment of the electrostatics in the micellar system which is often used as a simple model for the complex biological systems mentioned above.

Interfacial Ion Distribution. The connection between the micelle and the sodium counterions can be understood by investigating the distribution of all system components at the micelle–water interface (see Figure 3). Although it appears from Figure 1 that complete disassociation of all of the sodium ions from the micelle has been achieved with an average sodium to sulfur distance of 7.03 \AA , there is evidence from the sodium to sulfur radial distribution function (Figure 7) for the presence of “contact-ion pairs” in this system.

The first peak of the Na^+ –S radial distribution function reaches a maximum at a distance of 3.65 \AA . The slight ledge on the left side of this peak corresponds to regions of close contact between the sodium ions and sulfur. This most likely occurs due to favorable electrostatic interaction with three of the four headgroup oxygen atoms so that the sodium ion resides in the “pocket” formed by the tetrahedrally coordinated sulfur atom of the headgroup. It was also determined that throughout the last 4 ns of the simulation, an average of 25% of sodium ions are within the first shell of the micelle and 50% are within the first two shells.

An additional point of discussion regarding the distribution of the sodium ions around the micelle concerns the average

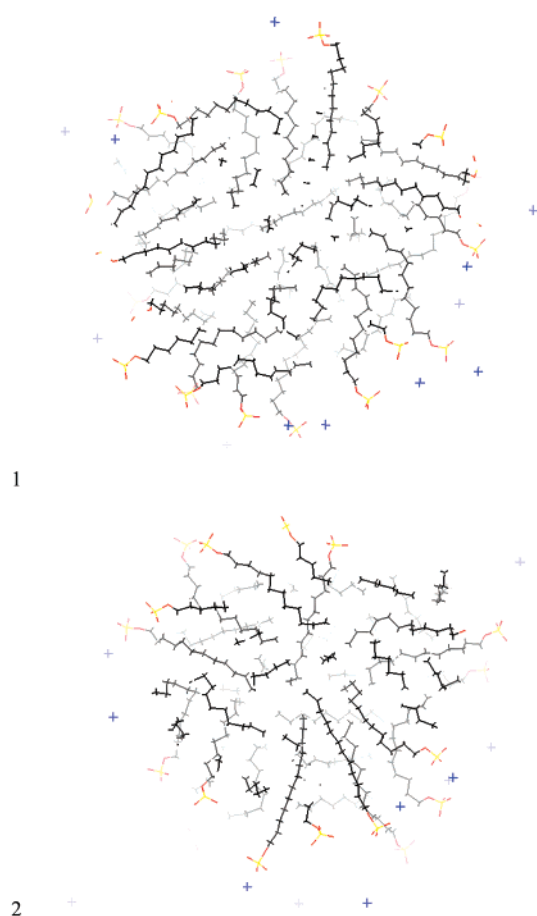


Figure 6. Micelle Cross Sections: (1) $t = 1 \text{ ns}$, (2) $t = 3 \text{ ns}$. Atoms are represented by the following colors: Blue = Sodium, Red = Oxygen, Yellow = Sulfur, Black = Carbon.

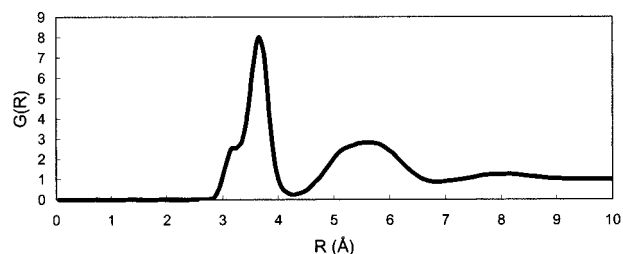


Figure 7. Sodium to Sulfur Radial Distribution Function.

distance of the sodium ions to the micelle center of mass (COM). From Figure 1, it appears that the sodium ions are 26.65 \AA from the COM. Comparing this value to the Na^+ –S distances obtained from Figure 7 of

$$\text{First Shell Na}^+ \text{ to micelle COM: } 19.6 \text{ \AA} + 4.25 \text{ \AA} = 23.85 \text{ \AA}$$

$$\text{Second Shell Na}^+ \text{ to micelle COM: } 19.6 \text{ \AA} + 6.80 \text{ \AA} = 26.40 \text{ \AA}$$

These values may at first seem contradictory to that from Figure 1, but determining the Na^+ –S average distance using the radial distribution function in Figure 7 gives a value of 7.03 \AA . This translates to an average distance from the sodium ions to the micelle center of mass of 19.6 \AA plus 7.03 \AA or 26.63 \AA , which is in excellent agreement with the value of 26.65 \AA obtained from Figure 1.

Sodium Bridging. A knowledge of the distribution of the sodium ions can be further refined by examining the number

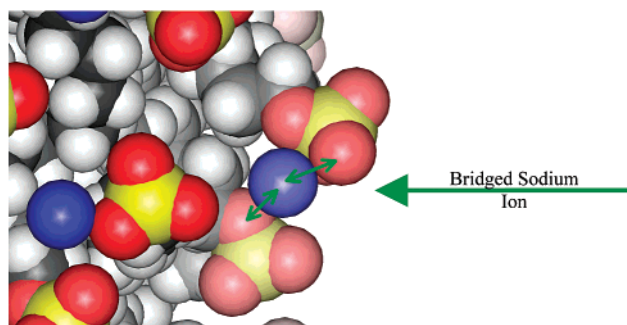


Figure 8. Sodium Bridging. Atoms are represented by the following colors: Blue = Sodium, Red = Oxygen, Yellow = Sulfur, Dark Gray = Carbon, Light Gray = Hydrogen.

TABLE 2: Sodium Diffusion Coefficient

shell	D (cm ² /s)
first shell	$1.0 \pm 0.2 \times 10^{-5}$
second shell	$1.4 \pm 0.2 \times 10^{-5}$
third shell	$1.9 \pm 0.1 \times 10^{-5}$
single Na ⁺ ion	$2.2 \pm 0.4 \times 10^{-5}$

of surfactant headgroups with multiple sodium ions in the first shell. This is hereafter referred to as sodium bridging. Figure 8 illustrates this phenomenon, showing a sodium ion that is in the first shell and bridging between two surfactant headgroups. Sometimes, a sodium ion is located in the first shell of three monomers through favorable interaction with the negatively charged oxygens of the three headgroups. Of the sodium ions that are in the first shell of headgroups, 72% are interacting with only one headgroup, whereas 23% are bridging two headgroups and only 5% are bridging three headgroups. These results indicate that contact ion pairs exist in SDS/water systems and that interactions between single counterions and multiple headgroups occur.

Sodium Diffusion. Using Einstein's equation, the diffusion coefficient of the sodium ions can be calculated

$$D = \lim_{t \rightarrow \infty} \frac{\langle r(t) - r(0) \rangle^2}{6t} \quad (3)$$

where D is the diffusion coefficient, and $r(t)$ is the displacement for time t . To determine the mobility of the counterions as a function of distance from the surface of the micelle, the sodium ions were categorized as first shell, second shell, or third shell based on the sodium to micelle oxygen radial distribution function (not shown). The diffusion coefficient for each of these groups was then found. All values are listed in Table 2 including that from a 300 K, 2910 ps NVT simulation of a single Na⁺ ion in a $24.9 \times 24.9 \times 24.9$ Å box of 512 waters. Error ranges were obtained by determining the diffusion coefficient for 22 separate 20 ps segments, averaging those, and finding the standard deviation. It must also be noted that the water model being used here is TIP3P, which typically gives a self-diffusion coefficient approximately twice that of the experimentally determined diffusion coefficient of water ($D_{\text{TIP3P}} = 5.4 \times 10^{-5}$ cm²/s.^{33,43,44}

These calculations show that the value of D for ions in the third shell from the simulation ($D = 1.9 \pm 0.1 \times 10^{-5}$ cm²/s) is within statistical error of that found in the single Na⁺ simulation ($D_{\text{Na}^+} = 2.2 \pm 0.4 \times 10^{-5}$ cm²/s). Subsequently, there is a decrease in the diffusion coefficient of sodium ions in the second shell ($D_{\text{second shell}} = 1.4 \pm 0.2 \times 10^{-5}$ cm²/s) and in the first shell ($D_{\text{first shell}} = 1.0 \pm 0.2 \times 10^{-5}$ cm²/s) compared to the ions in the bulk. The lower value of D for a single sodium

ion compared to pure water is due to the shell of water molecules that the sodium ion carries with it as it diffuses. For ions within the first shell of the micelle, the formation of contact-ion pairs with the headgroup limits the mobility of the ion.¹ We suspect that this is the primary mechanism for the decrease in the diffusion coefficient but realize that the geometry of the ion solvation shell controls much of the diffusion process as well. Previous simulations of ionic surfactant systems do not address the issue of counterion diffusion, only the location of the counterions as relates to the presence or absence of contact-ion pairs. Further in-depth analysis into the relative contributions of headgroup geometry, water solvation geometry, contact-ion pair formation, and friction to this decrease in sodium diffusion is necessary, and we would like to perform these studies in the future.

Conclusions

In the course of a 5 nanosecond molecular dynamics simulation, it has been determined that a micelle composed of 60 sodium dodecyl sulfate monomers and 7579 water molecules is stable. Of the micellar characteristics evaluated in this work, none had significant deviation over time except for the required equilibration time for the sodium counterion distribution. This was accounted for by discarding the first nanosecond of the production run. All micellar structural quantities were stable throughout the simulation.

Evaluation of the micelle shape by investigation of the moments of inertia along the axis and then computation of the eccentricity revealed that the micelle is not completely spherical, but has ellipsoidal components. In addition, the surfactant monomers are not all perfectly arranged around the center of the micelle, but, instead, liquification of the interior of the micelle allows torsional motion to assist the tails in orienting themselves in a variety of directions toward and away from the hydrocarbon core while still generally associating with the other tails.

The average radius of the micelle was 22 Å, whereas examination of the accessible surface area determined that the micelle contains a much larger surface area available to water molecules compared to a perfectly smooth ellipsoidal body. This implies a large amount of surface roughness. Hydrocarbon to water contact can be evaluated based on accessible surface area calculations. It has been found that approximately 70% of the water to micelle contact occurs via the headgroup, whereas there is a significant portion of available water to micelle contact occurring through the tails. Shelley et al. report that a number of terminal methyl groups make their way to the surface of the micelle during the course of a 182 ps production run. We also observe this phenomenon and attribute much of the accessible surface area contribution in the tail region to this behavior.

The sodium ions were found to form contact-ion pairs with the micelle headgroups rather than to be completely dissociated. This result differs from that of MacKerrell, primarily due to the differences in computational handling of long-range electrostatic forces. In this study, Ewald techniques were used, whereas truncation of the electrostatic shift and van der Waals switch smoothing functions were used in the MacKerrell work. Shelley et al did use Ewald techniques and did observe contact-ion pairs. Fifty percent of the counterions are in either the first or second shell, whereas the remainder are in the bulk compared to 35% in Shelley et al. For comparisons of sodium ion behavior in both previous simulations of SDS, the difference in simulation time must also be considered because we found that a full nanosecond was required for the sodium ions to reach an

equilibrium distribution. An observation by MacKerrell of an initial increase in the sodium ion distance to the micelle center of mass over the first 50 ps of the production run followed by an oscillation supports this conclusion. The diffusion coefficient for the ions in the third hydration shell (bulk) of the micelle was comparable to that found for a system containing Na^+ in water. In addition, the diffusion coefficients for the ions followed the pattern $D_{\text{bulk}} > D_{\text{second Shell}} > D_{\text{first Shell}}$. The presence of contact-ion pairs in the first shell supports this result, but further investigation into the exact origin of this pattern is necessary.

Acknowledgment. The authors would like to thank the North Carolina Supercomputing Center for allocation of computer time, the UNC-CH Supercomputing Center for use of their facilities, and the National Science Foundation (Grant No. 98-20793) for financial support. C.D.B. would also like to thank NSF's graduate fellowship program for funding.

References and Notes

- (1) Hedin, N.; Furo, I.; Eriksson, P. O. *J. Phys. Chem. B* **2000**, *104*, 8544.
- (2) Moren, A. K.; Nyden, M.; Soederman, O.; Khan, A. *Langmuir* **1999**, *15*, 5480.
- (3) Fremgen, D. E.; Smotkin, E. S.; Gerald, R. E.; Klinger, R. J.; Rathke, J. W. *J. Supercrit. Fluids* **2001**, *19*, 287.
- (4) Cerichelli, G.; Mancini, G. *Curr. Opin. Colloid Interface Sci.* **1997**, *2*, 641.
- (5) Van Gorkom, L. C.; Jensen, A. *Surfactant Sci. Ser.* **1998**, *73*, 169.
- (6) Closs, G. L.; Forbes, M. D. E.; Norris, J. R., Jr. *J. Phys. Chem.* **1987**, *91*, 3592.
- (7) Ottaviani, M. F.; Daddi, R.; Brustolon, M.; Turro, N. J.; Tomalia, D. *Appl. Magn. Reson.* **1997**, *13*, 347.
- (8) Glover, R. E.; Smith, R.; Jones, M. V.; Jackson, S. K.; Rowlands, C. C. *FEMS Microbiol. Lett.* **1999**, *177*, 57.
- (9) Earnshaw, J. C.; McCoo, E. *Langmuir* **1995**, *11*, 7155.
- (10) Kim, D.-H.; Oh, S.-G.; Cho, C.-G. *Colloid Polym. Sci.* **2001**, *279*, 39.
- (11) Bendedouch, D.; Chen, S. *J. Phys. Chem.* **1983**, *87*, 153.
- (12) Vass, S. *J. Phys. Chem. B* **2001**, *105*, 455.
- (13) Floriano, M. A.; Caponetti, E.; Panagiotopoulos, A. *Langmuir* **1999**, *15*, 3143.
- (14) Rodriguez-Guadarrama-L. A.; Talsania, S. K.; Mohanty, K. K.; Rajagopalan, R. *Langmuir* **1999**, *15*, 437.
- (15) Watanabe, K.; Ferrario, M.; Klein, M. *J. Phys. Chem.* **1988**, *92*, 819.
- (16) Shelley, J.; Shelley, M. *Curr. Opin. Colloid Interface Sci.* **2000**, *5*, 101.
- (17) Jonsson, B.; Edholm, O.; Teleman, O. *J. Chem. Phys.* **1986**, *85*, 2259.
- (18) Kuhn, H.; Rehage, H. *Prog. Coll. Polym. Sci.* **1998**, *111*, 158.
- (19) Kuhn, H.; Rehage, H. *Ber. Bunsen-Ges.* **1997**, *101*, 1485.
- (20) Kuhn, H.; Rehage, H. *Ber. Bunsen-Ges.* **1997**, *101*, 1493.
- (21) Kuhn, H.; Breitzke, B.; Rehage, H. *Colloid Polym. Sci.* **1998**, *276*, 824.
- (22) MacKerell, A. *J. Phys. Chem.* **1995**, *99*, 1846.
- (23) Tieleman, D. P.; van der Spoel, D.; Berendsen, H. J. C. *J. Phys. Chem. B* **2000**, *104*, 6380.
- (24) Shelley, J.; Watanabe, K.; Klein, M. *Int. J. Quantum Chem: Quantum Biol. Sym.* **1990**, *17*, 103–117.
- (25) Wendoloski, J. J.; Kimatian, S. J.; Schutt, C. E.; Salemme, F. R. *Science* **1989**, *243*, 636.
- (26) Bogusz, S.; Venable, R. M.; Pastor, R. W. *J. Phys. Chem. B* **2000**, *104*, 5462.
- (27) Bogusz, S.; Venable, R. M.; Pastor, R. W. *J. Phys. Chem. B* **2001**, *105*, 8312.
- (28) Marrink, S. J.; Tieleman, D. P.; Mark, A. E. *J. Phys. Chem. B* **2000**, *104*, 12 165.
- (29) Auffinger, P.; Beveridge, D. L. *Chem. Phys. Lett.* **1995**, *234*, 413.
- (30) Jonsson, B.; Lindman, B.; Holmberg, K.; Kronberg, B. *Surfactants and Polymers in Aqueous Solution*; West Sussex: John Wiley & Sons, 1998; p 53.
- (31) Essmann, U.; Perera, L.; Berkowitz, M. L.; Darden, T. A.; Lee, H.; Pedersen, L. *J. Chem. Phys.* **1995**, *103*, 8577.
- (32) Darden, T. A.; Perera, L.; Li, L.; Pedersen, L. *Structure* **1999**, *7*, R55.
- (33) Bruce, C. D.; Berkowitz, M. L.; Perera, L.; Forbes, M. D. E., in process, **2001**.
- (34) Chen, J. M.; Su, T. M.; Mou, C. Y. *J. Phys. Chem.* **1986**, *90*, 2418.
- (35) Schweighofer, K. J.; Essmann, U.; Berkowitz, M. *J. Phys. Chem. B* **1997**, *101*, 3793.
- (36) Case, D. A.; Pearlman, D. A.; Caldwell, J. W.; Cheatham, T. E., III; Ross, W. S.; Simmerling, C. L.; Darden, T. A.; Merz, K. M.; Stanton, R. V.; Cheng, A. L.; Vincent, J. J.; Crowley, M.; Tsui, V.; Radmer, R. J.; Duan, Y.; Pitera, J.; Massova, I.; Seibel, G. L.; Singh, U. C.; Weiner, P. K.; Kollman, P. A. *AMBER 6*, University of California, San Francisco, **1999**.
- (37) Berendsen, H. J. C.; Postma, J. P. M.; Van Gunsteren, W. F.; DiNola, A.; Haak, J. R. *J. Chem. Phys.* **1984**, *81*, 3684.
- (38) Salinal, S.; Cui, S.; Cochran, H.; Cummings, P. *Langmuir* **2001**, *17*, 1773.
- (39) Itri, R.; Amaral, L. Q. *J. Phys. Chem.* **1991**, *95*, 423.
- (40) Lee, B.; Richards, F. M. *J. Mol. Biol.* **1971**, *55*, 379.
- (41) Gelbart, W. M.; Bruinsma, R. F.; Pincus, P. A.; Parsegian, V.; Adrian, *Phys. Tod.* **2000**, *53*, 38.
- (42) Schreiber, H.; Steinhauser, O. *Biochemistry* **1992**, *31*, 5856.
- (43) van der Spoel, D.; van Maaren, P.; Berendsen, H. J. C. *J. Chem. Phys.* **1998**, *108*, 10 220.
- (44) Mark, P.; Nilsson, L. *J. Phys. Chem. A* **2001**, *105*, 9954.